International interlaboratory comparison of Raman spectroscopic analysis of CVD-grown graphene

Piers Turner, Keith Paton, Elizabeth Legge, Andres de Luna Bugallo, A Rocha-Robledo, Ahmed-Azmi Zahab, Alba Centeno, Alessio Sacco, Amaia Pesquera, Amaia Zurutuza, et al.

International Interlaboratory Comparison of Raman Spectroscopic Analysis of CVD-grown Graphene

Authors

Piers Turner[1], Keith R Paton[1], Elizabeth Legge[1], A. de Luna Bugallo[2], A.K.S. Rocha-Robledo[2], Ahmed-Azmi Zahab[3], Alba Centeno[4], Alessio Sacco[5], Amaia Pesquera[4], Amaia Zurutuza[4], Andrea Mario Rossi[5], Diana N.H. Tran[6,7], Diego L. Silva[8], Dusan Losic[6,7], Farzaneh Farivar[6,7], Hugo Kerdoncuff[9,10], Hyuksang Kwon[11], Jerome Pirart[12], João Luiz E. Campos[8], Kiran M Subhedar[13], Li-Lin Tay[14], Lingling Ren[15], Luiz Gustavo Cançado[8], Matthieu Paillet[3], Paul Finnie[16], Pei Lay Yap[6,7], Raul Arenal[12,17,18], Sanjay R Dhakate[13], Sebastian Wood[1], Sergio Jiménez-Sandoval[2], Tim Batten[19], Vaiva Nagyte[20], Yaxuan Yao[15], Angela R. Hight Walker[21], Erlon H Martins Ferreira[22], Cinzia Casiraghi[20], Andrew J. Pollard[1*].

Author affiliations

[1]National Physical Laboratory, Teddington, Middlesex, TW11 0LW, United Kingdom.

[2]Centro de Investigación y de Estudios Avanzados del IPN, Unidad Querétaro, Libramiento Norponiente No. 2000, Real de Juriquilla, Querétaro, Qro. C.P. 76230, Mexico.

[3]Laboratoire Charles Coulomb, CNRS, University of Montpellier, Montpellier 34095, France.

[4]Graphenea Semiconductor, Paseo Mikeletegi 83, 20009 Donostia-San Sebastian, Spain.

[5]National Institute of Metrological Research (INRiM), Strada delle Cacce 91, 10135 Torino, Italy.

[6]School of Chemical Engineering and Advanced Materials, The University of Adelaide, Adelaide, SA 5005, Australia.

[7]ARC Hub for Graphene Enabled Industry Transformation, The University of Adelaide, Adelaide, SA 5005, Australia.

[8]Departamento de Física, Universidade Federal de Minas Gerais, Belo Horizonte, MG, 30.123-970, Brazil.

[9]Danish Fundamental Metrology, Kogle Allé 5, 2970 Hørsholm, Denmark.

[10]NKT Photonics A/S, Blokken 84, 3460 Birkerød, Denmark.

[11]Korea Research Institute of Standards and Science, Daejeon 34113, Republic of Korea.

[12]Laboratorio de Microscopias Avanzadas (LMA), Universitad de Zaragoza, 50018 Zaragoza, Spain.

[13]CSIR-National Physical Laboratory, Dr K S Krishnan Marg, New Delhi 110 012, India.

[14]National Research Council Canada, Metrology Research Centre, Ottawa, ON K1A0R6.

[15]National Institute of Metrology, Beijing, 100029, China.

[16]National Research Council Canada, Security and Disruptive Technologies, 1200 Montreal Road, Ottawa, Ontario K1A 0R6.

[17]Instituto de Nanociencia y Materiales de Aragon (INMA), CSIC-Universidad de Zaragoza, 50009 Zaragoza, Spain.

[18]ARAID Foundation, 50018 Zaragoza, Spain.

[19]Renishaw Plc, New Mills, Wotton-under-Edge, Gloucestershire, GL12 8JR, United Kingdom

[20]Department of Chemistry, University of Manchester, Manchester, M139PL, United Kingdom.

[21]National Institute of Standards and Technology (NIST), Gaithersburg, MD, USA.

[22]National Institute of Metrology, Standardization and Technology (Inmetro), Rio de Janeiro, Brazil.

**andrew.pollard@npl.co.uk*

Keywords

Graphene, Raman spectroscopy, chemical vapour deposition, uncertainty, VAMAS, standardisation, interlaboratory study

Abstract

There is a pressing need for reliable, reproducible and accurate measurements of graphene's properties, through international standards, to facilitate industrial growth. However, trustworthy and verified standards require rigorous metrological studies, determining, quantifying and reducing the sources of measurement uncertainty. Towards this effort, we report the procedure and the results of an international interlaboratory comparison (ILC) study, conducted under Versailles Project on Advanced Materials and Standards (VAMAS). This ILC focusses on the comparability of Raman spectroscopy measurements of chemical vapour deposition (CVD) grown graphene using the same measurement protocol across different institutes and laboratories. With data gathered from 17 participants across academia, industry (including instrument manufacturers) and national metrology institutes, this study investigates the measurement uncertainty contributions from both Raman spectroscopy measurements and data analysis procedures, as well as provides solutions for improved accuracy and precision.

While many of the reported Raman metrics were relatively consistent, significant and meaningful outliers occurred due to differences in the instruments and data analysis. These variations resulted in inconsistent reports of peak intensity ratios, peak widths and the coverage of graphene. Due to a lack of relative intensity calibration, the relative difference reported in the 2D- and G peak intensity ratios ($I_{2\mathrm{D}}/I_{\mathrm{G}}$) was up to 200%. It was also shown that the standard deviation for Γ_{2D} values reported by different software packages, was 15× larger for Lorentzian fit functions than for pseudo-Voigt functions. This study has shown that by adopting a relative intensity calibration and consistent peak fitting and data analysis methodologies, these large, and previously unquantified, variations can be significantly reduced, allowing more reproducible and comparable measurements for the graphene community, supporting fundamental research through to the growing graphene industry worldwide. This project and its findings directly underpin the development of the ISO/IEC standard "*DTS 21356-2 - Nanotechnologies - Structural Characterisation of CVD-grown Graphene*".

1. Introduction

Graphene, first isolated in 2004 [1], is impacting many application areas such as solar cells, biosensors, thin-film transistors, composites, flexible electronics and energy storage [2-8]. This single layer of carbon atoms, with each atom bound to three neighbours in a honeycomb structure [9], has opened up an entire area of scientific research including a whole family of other 2D materials and their heterostructures [10-13]. As industrial uptake increases, reliable, accurate, and reproducible measurements of graphene are important to maintain quality in manufacture. In particular, many material properties such as the flake or grain size, thickness or number of layers and chemistry can vary depending on the production method and related processing parameters [14-19]. To this end, internationally standardised measurement protocols must be developed for graphene characterisation [20], so that technical data sheets for all graphene products globally have comparable measurands with well-understood uncertainties, regardless of their producer and/or production method. This will help ensure material quality throughout the supply chain, as well as allow informed decisions in terms of application requirements and health and safety.

Raman spectroscopy [21, 22] is a fast and non-destructive method that can provide structural, chemical and electronic information from a broad range of advanced materials. Today, most Raman spectrometers are coupled with an optical microscope and a translation stage enabling Raman mapping over a large area to study the variations in material properties across a sample. This technique has been used extensively in both fundamental and applied research for carbon-based nanostructures [23-31], and is also an invaluable industrial quality control (QC) method to detect structural damage, chemical modifications and unwanted by-products that may occur during manufacturing [32]. In the specific case of graphene, Raman spectroscopy is a very powerful tool due to the band structure of graphene, leading to resonant processes and strong electron-phonon coupling, which provide a strong Raman signal and unique features that can be used to characterise graphene. For example, Raman spectroscopy can provide an indication of the number of graphene layers [33-37], defects [38-41], strain [42, 43] and functionalisation [44].

The Raman spectrum of graphene consists of an array of characteristic peaks. The three main features discussed in this work are: the D peak (~1350 cm^{-1}), the G peak (~1580 cm^{-1}) and the 2D peak (~2700 cm^{-1}, also referred to as the G' peak). A representative Raman spectrum of single-layer graphene is shown in Figure 1a, which also illustrates the D' peak (~1620 cm^{-1}). The G band, which is observed in all sp^2 carbon systems, is due to the doubly degenerate zone centre E_{2g} mode [33], whereas the 2D and D bands originate from a second-order process, involving two phonons near the K point for the 2D band or one phonon and one defect in the case of the D band [23, 45]. The D band is due to the radial breathing mode of six-atom rings in the graphene lattice and requires a defect to be activated [23, 46], where defects are associated with symmetry-breaking regions in the lattice such as sp^3 defects, vacancy sites, as well as edges [47]. The 2D peak is the second order overtone of the D peak and has been commonly used to identify single-layer graphene, as a result of its unique electronic structure compared to Bernal/Rhombohedral few-layer graphene [33]. In this study, we will use the notation I for the maximum peak height (intensity), A for peak area, ω for the Raman shift of the peak centre, and Γ for the full width at half maximum (FWHM) of the peak. For example, I_{D} is the intensity of the D peak, A_{D} is the area of the D peak, ω_D is the peak position of the D peak, Γ_{D} is the FWHM of the D peak. Additionally, $I_{\mathrm{D}}/I_{\mathrm{G}}$ and $I_{2\mathrm{D}}/I_{\mathrm{G}}$, refer to the peak intensity ratio of the D peak and the G peak, and the peak intensity ratio of the 2D peak to the G peak,

respectively. For clarity, single-layer graphene, bilayer graphene and few-layer graphene will be specifically referred to as 1LG, 2LG and FLG, respectively.

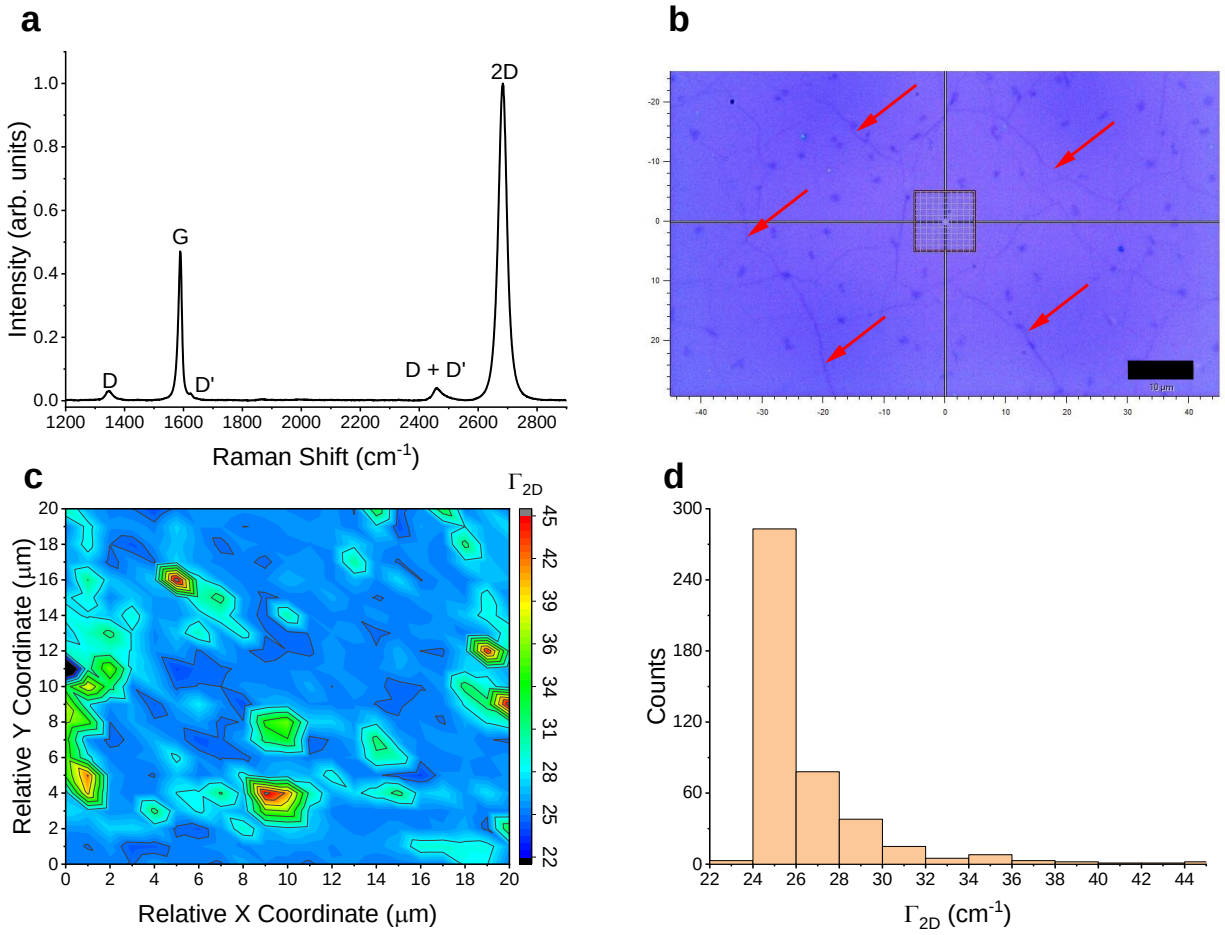

Figure 1: Representative images and data from a commercially-sourced, CVD-grown graphene sample on Si/SiO_2 that was used in this VAMAS interlaboratory study, using a 532 nm excitation laser with 0.83 mW power incident on the sample. (a) Raman spectra of CVD-grown graphene, normalised to the 2D peak intensity, showing the characteristic D- (1350 cm^{-1}), G- (1580 cm^{-1}), D'- (1620 cm^{-1}) and 2D Peaks (2700 cm^{-1}). (b) An optical image of the wrinkles (red arrows) in the CVD-grown graphene sheet viewed through a 100× objective, the scale bar is 10 μm. (c) A Raman map showing how the full width at half maximum (FWHM) of the Raman 2D (Γ_{2D}) peak varies across a 20 μm × 20 μm (1 μm step size) area near the edge of a CVD-grown graphene sheet. (d) A histogram showing the range of Γ_{2D} across the 20 μm × 20 μm area shown in (c) where the mean Γ_{2D} value is 27 cm^{-1} with a standard deviation of 3 cm^{-1}.

Although the Raman spectrum of graphene may be relatively simple, reliable interpretation of the spectra is nontrivial as it is sensitive to changes in multiple phenomena, including but not limited to electronic structure, defects, strain and doping. Furthermore, the changes in peak shapes/intensities can be small, and correlations between peaks and structural/chemical changes in graphene can be ambiguous. For example, depending on the amount of defects, a decreasing I_D/I_G ratio can suggest either an increasing or decreasing defect density. For a relatively small defect density, the I_D/I_G ratio increases with increasing number or area of defects, whereas for a much higher defect density, I_D/I_G decreases with increasing number or area of defects [38-41, 48]. For pristine graphene this occurs when the inter-defect distance approaches 5 nm [40]. These two stages can be distinguished by looking at additional Raman parameters, such as the Γ of selected peaks, because the Γ increases for increasing defect concentration [38, 39, 41] and strain [42, 43]. Directly comparing measurements between different instruments can also be challenging, as factors such as laser excitation energy [48, 49], laser power [50], instrument calibration, microscope objectives [51], slit

width and grating can affect Raman peak positions, peak widths and peak intensity ratios. An important example of this is the difference in the D peak position and intensity for the same graphene sample when using different excitation lasers, as it is strongly dispersive with excitation energy due to a Kohn Anomaly at K [48, 52-54]. Therefore comparisons can only be made directly for measurements using the same wavelength laser, whilst the laser power incident on the sample is also important due to issues with damage to the sample due to heating effects, which can also result in changes in peak position [55, 56].

Thus, an understanding of the measurement uncertainties for these Raman spectroscopy metrics, such as peak intensity ratios and widths is required. To improve confidence in Raman spectroscopic analysis of graphene, it is important to understand the variation in results obtained from different laboratories, using different equipment, conditions, and data analysis methodologies. To this end, rigorous interlaboratory comparison (ILC) studies are coordinated through VAMAS, with the results feeding directly into International Organization of Standardization (ISO) and International Electrotechnical Commission (IEC) committees, as these ILCs are a critical component in the adoption of international measurement standards. Several international graphene standards are under development within ISO TC229 'Nanotechnologies', jointly with IEC TC113. An example of a measurement standard is the recently published ISO/TS 21356-1:2021 'Structural characterisation of graphene — Part 1: Graphene from powders and dispersions' technical specification [57], which focuses on determining the physical properties of graphene present in powders and liquid dispersions. However, graphene sheets covering a substrate, are also important materials for different technological applications such as electronics [8].

Here, we present the results from the first ILC coordinated under VAMAS Technical Working Area (TWA) 41 'Graphene and Related 2D Materials' as Project 1 'Structural characterisation of CVD-grown graphene: Coverage on substrate, number of layers, level of disorder', jointly with VAMAS TWA 42 'Raman Spectroscopy and Microscopy'. The 17 participants that contributed to this study originated from 13 different countries and include representation from seven National Measurement Institutes (NMIs), five Universities, and two industrial participants.

The aim was to understand the uncertainties associated both with Raman measurements and Raman data analysis, before demonstrating solutions to reduce the variance observed, so this technique can be used across the whole graphene community to provide more accurate and precise results. Firstly, the method employed for this ILC will be described (section 2), before the results are reported with respect to (1) Raman peak intensity ratio (section 3.1), (2) Raman peak position (section 3.2) and (3) Raman peak width (section 3.3), along with methods to reduce the measurement uncertainty due to the issues observed.

These findings will ultimately directly support the development of the ISO/IEC standard "*DTS 21356-2 - Nanotechnologies - Structural Characterisation of CVD-grown Graphene*", which is currently under development in ISO TC229 and IEC TC113.

2. Methods

2.1 VAMAS Protocol and Participant Instrumentation

The VAMAS interlaboratory measurement protocol used for this ILC is appended to the Supplementary Information (SI). This includes instrumentation requirements, measurement protocols, data analysis procedures and reporting guidelines. Participants were required to use

Raman spectrometers that were capable of obtaining Raman maps, whilst operating with a backscattering (180°) geometry. As this ILC will be used as the basis of an international standard for industry, it is important to use commercially-available Raman spectrometers that are more typical of what would be used in a materials testing facility, whilst at the same time balancing the capability required to provide accurate results. To the same end, to compare the typically used methods of calibration available to different laboratories, the different participants were expected to at least perform a daily calibration using the 1st order Si peak of a silicon sample, but to record the overall calibration procedure used so they could be analysed alongside the data obtained. As many of the characteristic Raman peaks are dispersive with the laser photon energy [48, 58-60], the participants were also asked to use a laser with a wavelength of 532 nm (2.33 eV). If this was not possible, a laser wavelength of 514.5 nm (2.41 eV) was used instead, and in all cases the participants were asked to record the laser wavelength. Where possible the participants were also asked to use a 100× objective, but there were no specific requirement of numerical aperture (NA). The instrumentation details for each participant are included in Tables S1-1 and S1-2.

2.2 CVD-grown Graphene Sample

There is currently no certified reference material for graphene and so a material that was representative of commercially-available CVD-grown graphene [61, 62] was produced using commercial copper foils as a catalyst in a cold walled CVD reactor (Aixtron BM). After the synthesis, a polymethyl methacrylate (PMMA) sacrificial support layer was spin coated onto the graphene-covered Cu foil. The Cu was etched using a ferric chloride containing solution. The film was cleaned with distilled water several times as well as an acid cleaning step and transferred onto a silicon wafer with a 300 nm oxide layer (Si/SiO_2). After transfer the PMMA was removed using solvents by placing the material in an acetone bath for 30 min followed by another 30 min in clean acetone and 15 min in isopropyl alcohol (IPA). Finally, the samples were dried with nitrogen. The wafer was then cut into 10 mm × 10 mm samples (one for each participant), before being sent to the Lead Participant (LP).

To minimise damage during transport, the samples were shipped securely in 1” wafer shippers (Entegris, USA). Before being mailed to the participants, each sample was checked by the LP with a series of optical images and Raman maps. From optical microscopy analysis, the graphene appeared to be a continuous sheet, with no large islands or tears where the underlying substrate was visible. The only topological features that were visible were the wrinkles and folds that are a common feature for CVD-grown graphene, as shown in Figure 1b. Due to differing thermal expansion coefficients between graphene and the metallic growth substrates such as copper [61], wrinkles can form when the graphene and substrate are cooled to room temperature. Additional wrinkles may also occur when the graphene is transferred onto another substrate. It is worth noting that the corners of all the samples were damaged where they had come into physical contact with the hemispherical base of the 1” wafer shippers. This caused holes and tears where underlying silicon wafer could be observed. However, this damage only extended up to 200 µm from the edge of the sample (Figures S1-3 and S1-4) and did not interfere with any of the measurements in this study.

The participants were each sent separate 10 mm × 10 mm samples from the same batch of CVD-grown graphene, along with the measurement protocol and instructions on how to find a suitable location near the edge of the sample using a coordinate system and a series of optical images. The location near the edge (within 500 µm) of the CVD-grown graphene sheet had been measured by the LP before it was despatched, to check the suitability of the sample. For this type of CVD-grown material, additional properties, such as the wrinkles (Figure 1b), tears and residual contaminants from the growth and processing can cause variations of the measured Raman metrics [63, 64].

2.3 Raman Spectroscopy Measurements

Due to these variations across the samples, mapping over large areas and averaging the Raman metrics is required to reduce the chance of variability due to sample inhomogeneity. The participants each performed a Raman map at two locations on the CVD-grown graphene sample: one area close to the edge of the sample and one area approximately the geometric centre of the sample. This protocol mimics the expected sampling for a 10 mm × 10 mm sample in ISO DTS 21356-2 [57], providing an understanding of the material across the sample and not just in one position.

Figure 1c shows the spatial variations in the fitted Γ_{2D} values across a 20 µm × 20 µm area of a CVD-grown graphene sample, where the step size of the measurement was 1 µm. Although the theoretical laser spot size for commercially-available Raman spectrometers, typically using green or red laser excitation, is a few hundred nanometres (using an objective with numerical aperture of ~ 0.9), the actual laser spot diameter may be up to 2 µm in lateral dimensions, as a result of different objectives used; the laser spot size of the instrument used to generate Figure 1 was measured as 0.8 ± 0.2 µm [65], as measured from a mechanically exfoliated graphene flake (Figure S1-1). A 1 µm step size is therefore a compromise for typical Raman spectrometers to provide a suitable number of spectra that are representative of the material. The mean Γ_{2D} value for Figure 1c was calculated as 27 cm^{-1} with a standard deviation of 3 cm^{-1}. It should be noted that this standard deviation is comparable to the wavenumber resolution of typical Raman spectrometers and so care should be taken when comparing peak width measurements between instruments and when assigning peak width measurements to physical material properties. The wavenumber resolution of the instrument used by the LP was determined to be 2.4 ± 0.6 cm^{-1} (SI Section 1.2.4).

An investigation with a large 110 µm × 110 µm (1 µm step size) Raman map (Figure S4-1 and S4-2) demonstrated that by averaging Raman metrics over an area of at least 10 µm × 10 µm (121 spectra), localised material differences are significantly suppressed. The mean relative difference between the large area map and 100 randomly positioned 10 µm × 10 µm sub-maps was found to be (1.5 ± 1.2) % for Γ_{2D} and (3.1 ± 2.2) % for I_{2D}/I_G values (Figure S4-3). While the relative difference can be decreased by increasing the map size, this will significantly increase the measurement and analysis time, and only results in a limited improvement in relative difference. This suggests that performing Raman maps of 10 µm × 10 µm (121 spectra) is a reasonable compromise of time versus precision. However, for samples with greater spatial variations in the material properties, larger Raman maps with more Raman spectra are required to provide a representative distribution [66].

Each participant measured Raman maps by collecting Raman spectra over a 10 µm × 10 µm area with a 1 µm step size (121 total Raman spectra in each Raman map) for each of the two locations (edge and centre). The Raman spectra were measured with a wavenumber range of at least 1200 – 2900 cm^{-1}, an incident laser power of less than 1 mW measured at the focus, and an acquisition time of 5 seconds. However, if this did not produce spectra where the G peak intensity was at least ten times greater than the peak-to-peak variation in the background noise, the acquisition time was recommended to be increased up to a maximum of 30 seconds, in order to still avoid damage to the CVD-grown graphene through localised heating effects [40, 67]. Before each Raman map was collected, the objective lens position was first optimised by performing a series of Raman spectroscopy measurements about the optical focus (± 1 µm) and finding the focus position in which the highest Raman peak intensities were recorded. Depending on the measurement location and the calibration of the instrument the highest peak was either the Raman 2D peak or G peak. With these specific measurement requirements, all participants were able to produce Raman spectra with well-defined D-, G- and 2D Peaks (Figure S2-1 to Figure S2-17).

2.4 Raman Spectroscopy Data Analysis

When processing the acquired data, the protocol stipulates that the Raman maps should first be baseline corrected with a linear baseline and then the D-, G- and 2D peaks fitted with a Lorentzian lineshape. Note that while most participants used a linear baseline, participants #4, #5, #7, #8 used non-linear (e.g. polynomial) baselines. Using the resulting parameters from these peak fits, the participants were asked to report key Raman metrics, namely A_{G}, $I_{\mathrm{D}}/I_{\mathrm{G}}$, $I_{2\mathrm{D}}/I_{\mathrm{G}}$, Γ_{G} and $\Gamma_{2\mathrm{D}}$, along with a calculation of the graphene coverage (1LG/2LG/FLG) and the 1LG graphene coverage. The Raman metrics from the 121 spectra in each Raman map were averaged before being compared with the Raman metrics from the other participants. As there are a significant number of metrics that can be compared, only the $I_{2\mathrm{D}}/I_{\mathrm{G}}$ ratio and the $\Gamma_{2\mathrm{D}}$ are explored in detail here due to their significance in the graphene community. However, the supplementary information contains a comparison of many more Raman metrics for graphene (Table S3-4 to S3-24).

As the CVD-grown graphene material that was used in this ILC study was transferred on to an Si/SiO_2 substrate with a 300 nm oxide layer, the 1LG peak is expected to have a 2D Peak that is a single symmetrical peak with a Lorentzian line shape and $\Gamma_{2D} \leq 35$ cm^{-1} [60, 61, 68, 69]. It should also be noted that some stacking orders between consecutive graphene layers in multiple layers of graphene can also produce 2D peak widths of ≤ 35 cm^{-1} [70]. The $I_{2\mathrm{D}}/I_{\mathrm{G}}$ ratio has also been proposed to identify 1LG: for pristine 1LG, $I_{2\mathrm{D}}/I_{\mathrm{G}}$ is typically >2 [20]. However, this ratio can be reduced by several factors, including stacking order between consecutive graphene layers [71, 72], defects [38, 73], doping [59], interference effects [49, 74] and the proximity to the edge of the CVD-grown graphene sheet [75]. Therefore, it cannot be conclusively used to indicate the presence of 1LG and it is challenging to quantify the number of graphene layers from the Γ_{2D} and $I_{2\mathrm{D}}/I_{\mathrm{G}}$ ratio. For the purposes of this ILC determining the causes of uncertainty and irreproducibility, the process of determining the number of graphene layers was estimated from the FWHM of the 2D peak, using a value of 35 cm^{-1} as a threshold between 1LG and 2LG. This threshold value was chosen from previous work on similar material [60, 61, 68, 69, 76] and is not necessarily applicable to other materials.

Due to limitations in determining the number of graphene layers using Raman spectroscopy alone, Transmission Electron Microscopy (TEM), Atomic Force Microscopy (AFM) or optical microscopy should be performed to complement observations from the Raman spectroscopy results [57]. To this end, the ISO standard under development to determine the structural properties of CVD-grown graphene, ISO DTS 21356-2, requires Raman spectroscopy measurements of the material under investigation as well as complementary optical microscopy and TEM measurements to confirm the conclusions with regard to the number of layers. As the G peak is characteristic of graphitic materials, the presence of the G peak In Raman spectra was used to estimate the coverage of CVD graphene. This was undertaken by attributing pixels with A_G greater than 10 % of the average G peak area across the Raman map as areas where one or more layers of graphene are present [20]. As a Raman G-peak could still be detected if any holes in the CVD graphene sheet were smaller than the laser spot size, the resulting graphene coverage values are likely to be over estimated. Pixels that were recorded as having graphene layers present, but were not specifically 1LG, were recorded as having a thickness of greater than one layer.

2.5 ILC Analysis of Participants' Results

As illustrated in a flow chart of the datasets in this study (Figure 2), after the ILC measurements were performed, the participants returned the CVD-grown graphene sample to the LP, as well as a measurement report containing their measurement details and the calculated Raman metrics which

they produced from their Raman maps, as well as providing the raw, unprocessed Raman spectra. After receiving the samples and data back from the participants, the LP analysed the participants' raw spectra (see section 1.2.2 in the SI for details). To provide a direct comparison of the results from different participants as well as to help negate the variation in the results due to differing properties of the CVD-grown graphene on the microscale, the areas that were measured by each participant were remeasured by the LP. However, in some cases, it was not possible to conclusively identify and measure exactly the same area of sample after the sample had been returned to the LP, as some participants did not have high resolution cameras on their instruments, making it difficult to locate the areas they measured. Therefore, all quantitative comparisons and calculations of uncertainty have been determined using only the data where there is a direct comparison available (using the participant and LP results) of the same area.

Therefore, for each measurement location (edge and centre) there were ultimately 3 distinct datasets that were compared: participant-measured and participant-processed (PM-PP), participant-measured and lead-participant-processed (PM-LP), and lead-participant-measured and lead-participant-processed (LM-LP), as shown in Figure 2.

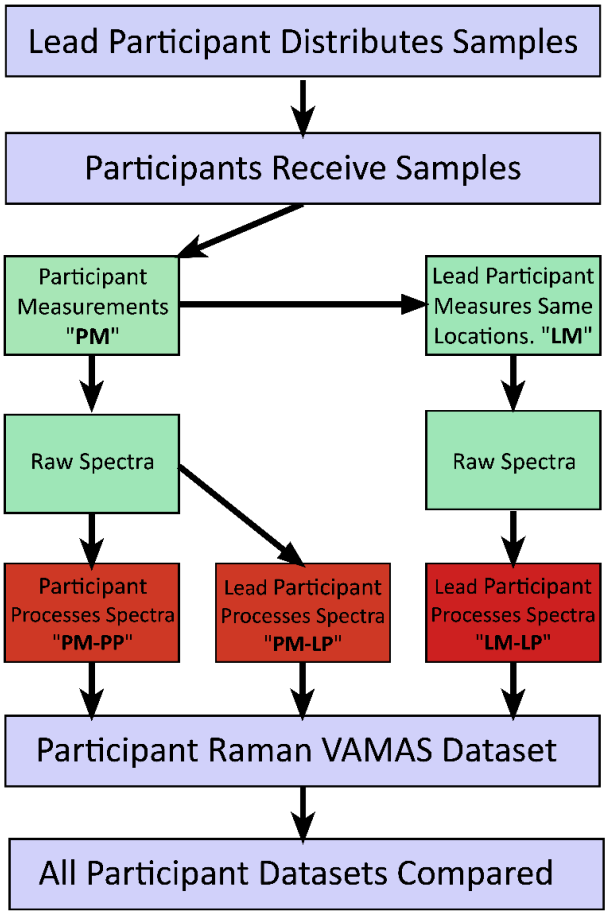

Figure 2: A flow chart showing how the measurements (green boxes) and data analysis (red boxes) were performed by the participants and the LP in this Raman VAMAS interlaboratory study. As measurements were carried out at both the edge and the centre of CVD-grown graphene sample, there are 6 total datasets per participant (edge PM-PP, PM-LP, LM-LP and centre PM-PP, PM-LP, LM-LP).

To explore how variations in data analysis (*e.g.* cosmic ray removal, background subtraction, peak fitting) affect the reported Raman metrics, the LP processed the participants raw spectra and compared the resulting metrics (PM-LP) with those reported by the participants (PM-PP). To

understand how differences in measurement hardware and instrument calibration can influence the reported Raman measurements, the LP re-measured the same areas of interest as the participants and compared the resulting Raman metrics (LM-LP) with the participants' results (PM-LP).

For each Raman metric (for example I_{2D}/I_G and Γ_{2D}) the mean value was calculated for each Raman map (from the 121 spectra taken for each map). This was done for the each of the two Raman maps produced by each participant (edge and centre). The relative difference between the participants' results and the corresponding results from the LP was then calculated:

$$\Delta_i\ (\%) = \left(\frac{V_{(i,\mathrm{P})}}{V_{(i,\mathrm{L})}} - 1\right) \times 100 \qquad (1)$$

Where i is the Raman metric, Δ_i is the relative difference in the mean value of a given metric (e.g. Δ_{I_{2D}/I_G}), $V_{(i,\mathrm{P})}$ is the participant's mean Raman metric value and $V_{(i,\mathrm{L})}$ is the LP's corresponding mean Raman metric value.

To then quantify the overall mean difference for each metric across all participants, the root mean square error (RMSE) for each metric has been calculated:

$$RMSE_i = \sqrt{\frac{\sum_{j=1}^{N}\left(V_{(j,\mathrm{L})} - V_{(j,\mathrm{P})}\right)^2}{N}} \qquad (2)$$

Where i is the Raman metric, j is the participant number, $V_{(j,\mathrm{L})}$ is the Lead Participant's Raman metric value, $V_{(j,\mathrm{P})}$ is the participant's Raman metric value and N is the number of comparable Raman metric values. These *RMSE* values are shown in Supplementary Information (Tables S3-3 to S3-23).

While the PM-PP and PM-LP datasets are directly comparable, as they originate from the same Raman map, the PM-LP and LM-LP datasets can only be reliably compared when the Raman maps were measured at the same location by both the participant and the LP. Due to material differences (e.g. wrinkles and tears) across the CVD-grown graphene, a slight variation in the sample measurement location between the participant and the LP could result in the Raman metrics being skewed. If the Raman maps measured by the participants had a strong resemblance to the Raman maps from the same area measured by the LP, they were considered to have good alignment (Figure S8-1 to Figures S8-17). In total, 25 out of the 34 Raman maps measured by the participants were found to have a good alignment with the LP Raman maps. Only data from these 25 well-aligned maps were compared when calculating the *RMSE* for measurement differences, whereas all 34 maps were compared when calculating the *RMSE* for data analysis differences.

3. Results and Discussion

Raman spectrometers from 5 different manufacturers were used to collect the Raman spectra and 7 different software packages were used to process and fit the data. While some participants used the software that was supplied with their Raman spectrometer to process the Raman data, others used custom developed software tools such as LabVIEW, MATLAB and Python. Most participants used a 532 nm laser and 100× optical objective lens, as called for in the protocol. The most common NA was 0.9 and all participants reported using an incident laser power below 1 mW. Although the VAMAS protocol suggested using a Lorentzian function for peak fitting, participant #13 used a pseudo-Voigt

function as it appeared to have a better fit with the data. Lastly, all participants regularly calibrated the peak positions of their spectrometers using a reference sample, such as a silicon wafer. Only two participants reported calibrating the spectral response function with a calibrated light source (e.g. a halogen lamp or white light source) to correct for the spectrometer sensitivity at different energies [77]. Table S1-1 in the Supplementary Information, has a full list of the instruments and software packages featuring in this study.

A series of optical images of the CVD-grown graphene samples were obtained before they were sent to participants making it possible to determine if the samples had been damaged during transport. While a small number of samples were found to have visible changes when they were returned to the LP (Figure S1-5), the optical images showed the original measurement locations remained intact. As such, the areas that were measured by the participants could be, on the most part, located and re-measured by the LP. While the participants were asked to measure Raman images from both the edge and the geometric centre of the sample, for simplicity only the centre measurements will be presented in Figures 3 and 4, with more analysis of the edge areas included in Section 5 of the SI. It is worth noting that the Γ_{2D} is consistently 10 % greater (~3 cm^{-1}) at the centre of the CVD-grown graphene sheet compared to the edge (Figure S5-21). This difference is likely due to strain at the centre of CVD-grown graphene sheet, which has been released at the edges of the sample due to the original wafer being cut into multiple samples [78]. For completeness, the tables in the SI show the raw data and relative differences from the edge, the centre and across both measurement areas combined.

Table S3-1 and Table S3-3 show a summary of the relative differences, absolute differences and root mean square error due to data analysis and measurements, respectively.

3.1. Peak Intensity Ratio

I_{2D}/I_G Peak Intensity Ratio

Figure 3a shows the peak intensity ratio, I_{2D}/I_G measured by each participant, with data analysis performed by either the participant (PM-PP) or the LP (PM-LP). As the Raman measurements presented in Figure 3a were performed by the participants, any resulting variance in I_{2D}/I_G between the participants and the LP is due to differences in data analysis methodologies. Most participants reported a mean I_{2D}/I_G ratio between 1 and 3, however participant #2 reported an I_{2D}/I_G ratio of ~ 6. The data in Figure 3a shows that the $RMSE_{I_{2D}/I_G}$ due to analysis is ~0.03. This suggests that the data analysis methodologies used by the participants (cosmic ray removal, background subtraction and peak fitting) are relatively consistent with the LP, and the resulting I_{2D}/I_G ratios are not significantly affected by the data analysis methodology/software tools used by the participants.

To study the differences due to the measurement, the same area of interest that was measured by the participant was re-measured by the LP and the datasets compared; this compares differences in instrument hardware and calibration. The I_{2D}/I_G ratios reported by the participants (PM-LP) and the LP (LM-LP) from the same areas are shown in Figure 3b. To mitigate any differences caused by data analysis methodologies, the participants' unprocessed Raman spectra was processed by the LP and compared with the LP's measurements from the same area of interest.

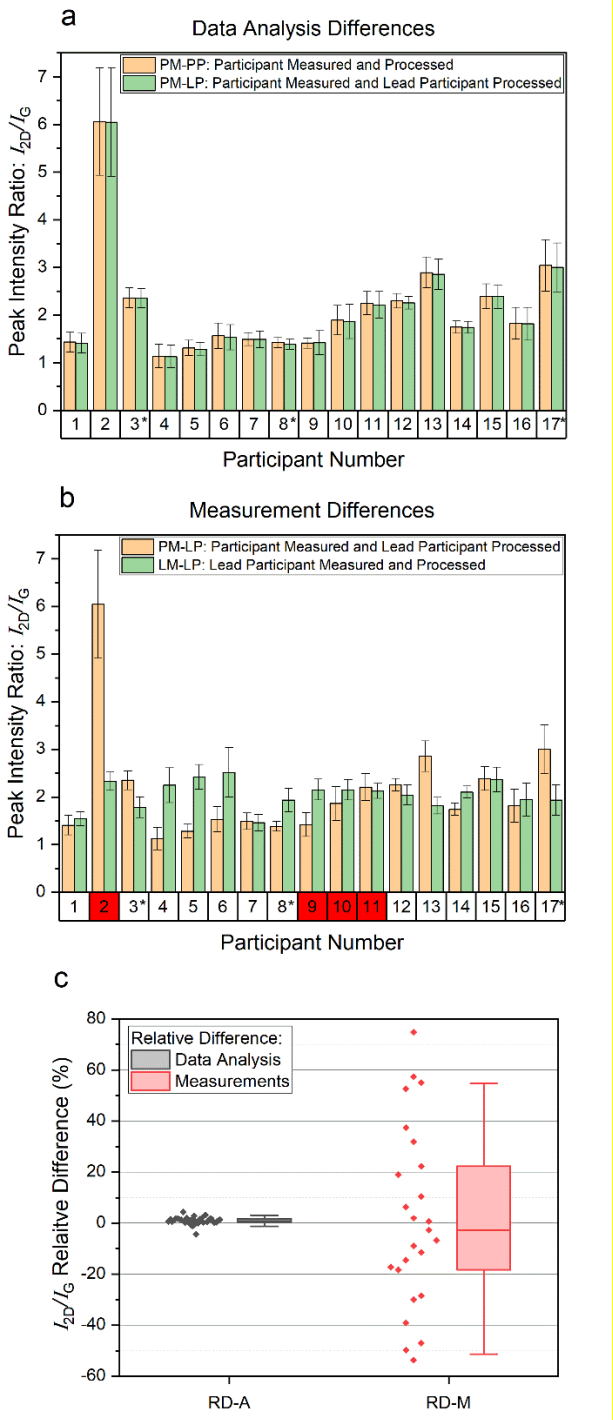

*Figure 3: The mean Raman peak intensity ratios, I_{2D}/I_G measured from a 10 µm × 10 µm area (121 spectra) at the centre of a CVD-grown graphene sheet on a Si/SiO_2 substrate. All peaks were fitted with a Lorentzian function except participant #13 who used a pseudo-Voigt function. Participants used a 532 nm laser, other than three participants who used a 514.5 nm laser, as denoted with an *. By comparing I_{2D}/I_G measurements from the participants and the LP dataset, differences that arise due to data analysis methodologies and the measurements themselves can be highlighted. (a) shows how the I_{2D}/I_G ratios are affected by differences in the data analysis, and (b) shows how the I_{2D}/I_G ratios are affected by differences in the measurement, with participant numbers labelled as red if the participants' and LP's measurement locations were classed as not well aligned. The error bars for (a) and (b) are the standard deviation in the I_{2D}/I_G ratios within each Raman map. (c) A box plot showing the relative difference in I_{2D}/I_G ratios (Δ_{I_{2D}/I_G}) due to data analysis (RD-A) and measurements (RD-M); the RD-M data excludes Δ_{I_{2D}/I_G} values from Raman maps that are not well aligned. Each box shows the 25th, 50th (median) and 75th percentiles, and the whiskers show the standard deviation multiplied by 1.5. The raw data is also shown as data points, randomly offset on the X-axis in a way to allow ease of viewing. The raw data for this figure is in Table S3-4.*

Figure 3c shows that there is a significantly larger distribution of Δ_{I_{2D}/I_G} values for measurement differences than for data analysis differences. As participant #2 reported that their Raman spectrometer was specifically optimised for infrared Raman measurements, the large variation in the reported I_{2D}/I_G with the LP (> 200 %) is likely related to a non-linear intensity response in the visible range. Even though participant #2's Raman measurements were not well aligned with the LP, and are therefore excluded from the $RMSE_{I_{2D}/I_G}$ statistics, such a larger I_{2D}/I_G ratio would not be expected when compared to the other areas measured for this sample of CVD-grown graphene on a Si/SiO_2 substrate. This outlier clearly demonstrates that the comparison of peak intensity ratios between instruments can be misleading without an understanding of how the value was obtained. The $RMSE_{I_{2D}/I_G}$ values from all participants were 0.031 for data analysis and 0.69 for measurements (Table S3-3). Because the peak area scales with the peak intensity, the A_{2D}/A_G peak area ratios showed a similar result in the $RMSE_{A_{2D}/A_G}$ values to the I_{2D}/I_G peak intensity ratios: 0.3 for data analysis and 1.2 for measurements. While the LP reported I_{2D}/I_G ratios of ~2 across most samples, the participants reported more varied I_{2D}/I_G ratios of between ~1 and ~4 (excluding participant #2), even for directly comparable data measured at the same positions of the sample.

As spectrometers have differences in their wavelength-dependant optical transmission characteristics and the quantum efficiency of their optics and detectors (Figure S6-1), spectra captured from different Raman spectrometers will show variations in measured peak intensity ratios and peak areas if these effects have not been corrected [49, 75]. The error in the recorded spectral intensity can be especially pronounced in peaks that have large differences in Raman shift between them, such as the G peak and the 2D Peak [49]. This variance can be corrected using either calibrated light sources with defined spectral output, such as the sources used by participant #6 and #14, or by using Standard/Certified Reference Materials (SRMs / CRMs). In this study the LP used SRM (2242a) from the National Institute of Standard and Technology (NIST) [79]. The two participants that carried out relative intensity corrections reported the lowest $RMSE_{I_{2D}/I_G}$ values (Table S6-3), which demonstrates that the large value of $RMSE_{I_{2D}/I_G}$ for measurement differences is caused by a lack of instrument intensity-wavelength response calibration, clearly showing the need for this type of calibration to allow comparable Raman spectroscopy data from more than one instrument.

However, it should be noted that relative intensity calibration with calibrated light sources have practical challenges: they require periodic re-calibration and may require additional optical components such as an integrating sphere [80]. In contrast, SRMs are secondary emission standards that are luminescent with laser irradiation, and this luminescence can be calibrated against primary light source standards to provide a source of known relative irradiance. These luminescent glass standards have advantages over calibrated light sources as they require no additional equipment, do not require periodic re-calibration, and account for the entire length of optical path in the Raman spectrometer. However, these SRMs can be expensive, are often out of stock, and a different reference material is required for each laser wavelength.

When applying a relative intensity correction to the LP's Raman spectrometer, the peak intensity ratio, I_{2D}/I_G, increased by ~10 % and the I_D/I_G ratio increased by ~ 8 % (Table S6-1). However, in triple-grating monochromator Raman spectrometers the correction factor can be much higher, as shown in Klar *et al.* [49, 81]. Details on the relative intensity calibration carried out by the LP and participants #6 and #14 are included in Section 6.2 in the Supplementary Information.

I_D/I_G Peak Intensity Ratio

As well as I_{2D}/I_G, the participants were also asked to report the I_D/I_G ratio, which is indicative of the level of disorder. The CVD-grown graphene samples used in this study had a low level of disorder and the resulting D peaks in the graphene spectra had a consistently low relative intensity compared to that of the G peak, with the D peak occasionally indistinguishable from the background noise (Figure S2-1 to Figure S2-17). The mean I_D/I_G reported by the participants and the LP from well aligned Raman maps was (0.06 ± 0.06) and (0.13 ± 0.01), respectively. However, fitting peaks with low absolute intensities can result in substantial fitting errors; the mean R-Squared value for the D peak, G peak and 2D peaks fits across all the spectra measured and processed by the LP in this ILC was 0.6 ± 0.3, 0.990 ± 0.009 and 0.996 ± 0.005, respectively. The RMSE value due to data analysis was 0.031 for I_D/I_G.

In some cases, large relative differences can occur due to fitting errors. For example, some participants reported negative peak intensities, which were clearly erroneous. These findings show that peak fitting bounds should be carefully applied to mitigate erroneous and non-physical peak fits, especially when attempting to fit peaks with low absolute intensities. In the case where clearly erroneous peak fits occur, standardised methods should describe that these data should be removed from the statistics.

3.2. Peak Position

While many participants did not calibrate their instrument intensity response functions, all participants reported frequent Raman spectral calibrations using reference samples such as silicon, Teflon, polystyrene, cyclohexane, highly oriented pyrolytic graphite (HOPG), and AgNe or HgAr lamps (Table S1-1) [82]. The consistency of these wavelength calibrations was explored by comparing the peak position of the characteristic D-, G- and 2D Raman peaks measured by the different participants. As the participants were not required to calculate the peak positions in the VAMAS protocol, this analysis directly compares relative differences in spectral calibration between the LP and participants instruments through analysis of the participants and LP raw data by solely the LP. In the aligned Raman maps measured with a 532 nm laser the relative difference in peak position was less than 0.3% for all peaks, and the RMSE values for the D-, G-, and 2D peak positions were 5.7 cm^{-1}, 3.3 cm^{-1} and 2.9 cm^{-1}, respectively. These results demonstrate that the wavelength calibrations procedures employed by the participants result in relatively consistent peak position measurements of the characteristic Raman D-, G-, and 2D Peaks across all participants, but with a non-negligible uncertainty of at least 3 cm^{-1} that should be considered when comparing Raman spectroscopy studies of graphene.

However, as the D- and 2D peaks are dispersive with laser frequency (~50 cm^{-1}/eV for the D peak [58] and ~90 cm^{-1}/eV for the 2D peak [59]), it was expected that the D- and 2D peak positions would vary between participants that employed different laser wavelengths. Participants #3, #8 and #17 used a 514.5 nm wavelength laser (2.41 eV), whereas all other participants and the LP used a 532 nm (2.33 eV) wavelength laser. While the D peak position shifts varied inconsistently between the LP and the participants #3, #8 and #17 (- 2 cm^{-1} to 16 cm^{-1}), with the variability in the D peak position likely due to the uncertainty associated with fitting a low intensity peak. However, there were more consistent peak shifts for the 2D peak. When compared to the LP data, the 2D peak was consistently ~6 cm^{-1} higher for participants #3, #8 and #17, which is consistent with the expected peak shift of 7.2 cm^{-1} [59]. See Table S3-8 to Table S3-10 for a full breakdown of these peak position comparisons,

and how they compare to the spectral dispersions and laser wavelengths of the spectrometers used to measure them.

3.3. Peak Width

Figure 4 compares $\Delta_{\Gamma_{2D}}$ and how it is affected by differences in analysis methodologies and measurements. The $RMSE_{\Gamma_{2D}}$ value from all participants was 2.2 cm^{-1} for data analysis and 1.2 cm^{-1} for measurement differences.

When estimating the 1LG coverage from these Γ_{2D} values, the relative difference between the LP and the participants increases considerably. If a process of identifying the percentage of 1LG coverage versus a greater number of graphene layers is performed using Γ_{2D}, and Γ_{2D} for 1LG is assumed to be less than 35 cm^{-1}, the $RMSE_{1LG}$ values (for 1LG percentage coverage) across all participants were 27% for data analysis and 9.4% for measurements. However, these large 1LG coverage variations can be significantly skewed by small changes in the Γ_{2D} threshold value. Despite there being inconsistent reports of 1LG coverage, only 1 % of measurements found no evidence of 1LG/2LG/FLG when measured by either the participants or the LP (Table S3-10) as determined from the aforementioned A_G calculation. Such large differences in $RMSE_{1LG}$ due to data processing are especially concerning when considered in the context of using Raman spectroscopy as a quality control (QC) method for CVD-grown graphene.

Alongside the $RMSE_{\Gamma_{2D}}$ values, Figure 4c shows that there is a larger distribution of $\Delta_{\Gamma_{2D}}$ values due to data analysis than for measurements. Some variation in the relative differences due to measurements may be expected as a result of material damage during shipping, misaligned measurement areas and spectrometer differences (e.g. slit width and spectral resolution, for example between single and triple monochromators). However, the Raman maps used to calculate the relative difference due to data analysis are identical. Therefore, the larger relative differences due to data analysis are unexpected and need to be investigated further.

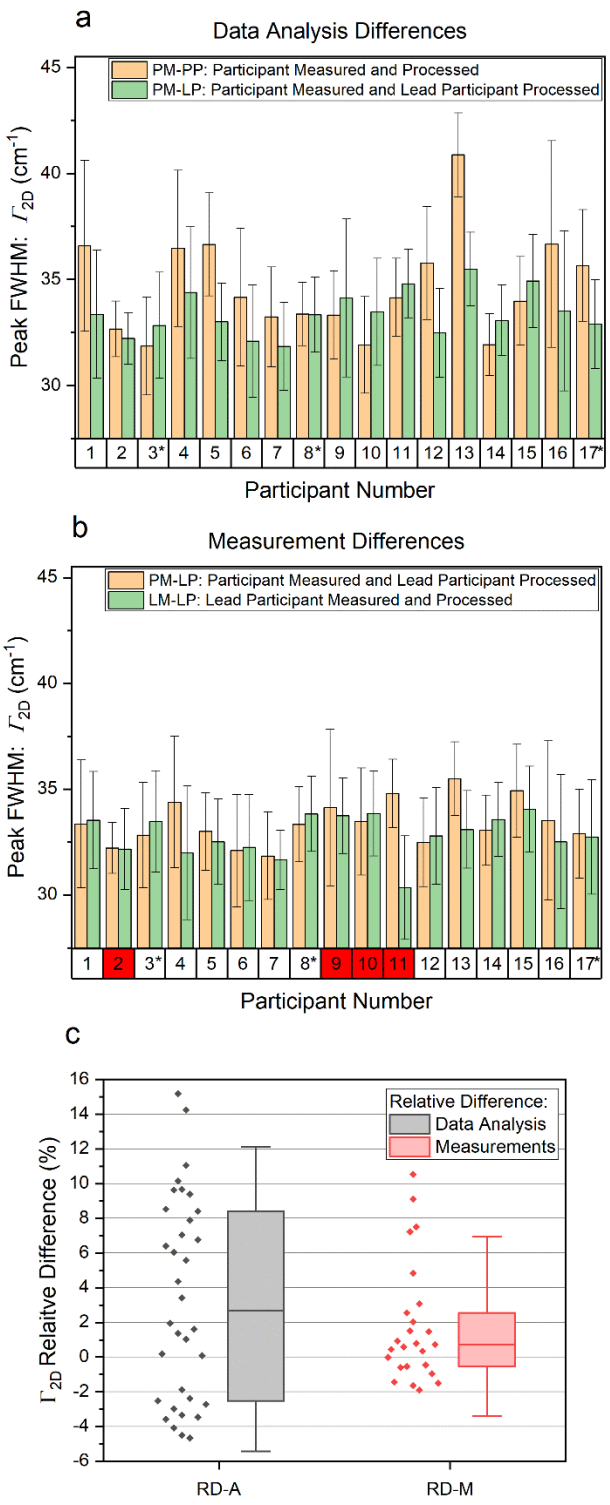

*Figure 4: The mean FWHM of the Raman 2D peak, Γ_{2D}, measured from a 10 µm x 10 µm area (121 spectra) at the centre of a CVD-grown graphene sheet on a Si/SiO_2 substrate. Participants used a 532 nm laser, other than three participants who used a 514.5 nm laser, as denoted with an *. By comparing Γ_{2D} measurements from the participants and the LP dataset, differences that arise due to data analysis methodologies and measurements can be separated. (a) shows how the Γ_{2D} values are affected by differences in the participant's analysis methodologies, and (b) shows how the Γ_{2D} values are affected due to differences in the measurements themselves, with participant numbers labelled as red if the participants' and LP's measurement locations were classed as not well aligned. The error bars for (a) and (b) are the standard deviation of Γ_{2D} from each Raman map. (c) A box plot showing the relative difference in Γ_{2D} ratios ($\Delta_{\Gamma_{2D}}$) due to data analysis (RD-A) and measurements (RD-M); the RD-M data excludes Δ_{I_{2D}/I_G} values from Raman maps that are not well aligned. Each box shows the 25th, 50th (median) and 75th percentiles, and the whiskers show the standard deviation multiplied by 1.5. The raw data is also shown as data points, randomly offset on the X-axis in a way to allow ease of viewing. The raw data for this figure is in Table S3-6.*

Peak Fitting Functions

Participant #13 used a pseudo-Voigt function rather than a Lorentzian function and some differences in peak metrics such as Γ_{2D} may be expected, as a pseudo-Voigt function is a linear combination (not a convolution) of Lorentzian and Gaussian curves [83]. To explore the effect of peak fit function on the relative difference due to data analysis, participant #13's data was re-fitted with a pseudo-Voigt function in OriginPro as used as for a comparison between the participant and LP data. Surprisingly, when using a pseudo-Voigt function, the resulting $\Delta_{\Gamma_{2D}}$ for participant #13 due to data analysis decreased by up to three orders of magnitude, to less than 0.05 % (Table S7-1) and the distribution in Γ_{2D} values were almost identical (Figure S7-1). Furthermore, these small relative differences occurred despite participant #13 and the LP using different software packages to analyse the Raman spectra; participant #13 used Witec Project FIVE and the LP used OriginPro 2020. These findings suggest that the Lorentzian peak function may produce inconsistent fit metrics when fitting Raman spectra from CVD-grown graphene on Si/SiO_2. To investigate this further, the same Raman map was fitted with a Lorentzian and a pseudo-Voigt function separately in a variety of common software packages for processing Raman data.

Before fitting, the Raman map was pre-processed by removing signals due to cosmic rays and then performing background subtraction and normalisation in WiRE (Renishaw). When fitting the Raman D-, G- and 2D Peaks, each peak was isolated from the spectrum, with a window of ± 100 cm^{-1} either side of the centre of the peak, and then fitted using a consistent set of fitting constraints (Table S1-3). Isolating each peak from the spectrum ensured the fitting optimisation of each peak was carried out independently. Details of these fitting constraints and software details are supplied in Section 1.2.2 in the Supplementary Information. A pseudo-Voigt function (Eq. 3) was chosen instead of a Voigt function as it is simpler to fit and it allows the ratio of Lorentzian and Gaussian components to be quantified.

$$y = y_0 + A\left[m_u \frac{2}{\mu}\frac{w}{4(x-x_c)^2} + (1-m_u)\frac{\sqrt{4ln2}}{\sqrt{\pi}w} e^{-\frac{4ln2}{w^2}(x-x_c)^2}\right] \quad (3)$$

Where y_0 is the background, A is the pseudo-Voigt peak area, w is the pseudo-Voigt FWHM, x_c is the pseudo-Voigt peak centre, and m_u is the profile shape parameter; this pseudo-Voigt function originates from OriginPro 2020 ("PsdVoigt1"). For a peak with an increasing Gaussian component, m_u shifts from 0 to 1. As WiRE (Renishaw) and Labspec (Horiba) do not allow fitting with user specified peak functions, a "mixed" and "GaussLoren" peak fitting function was used in WiRE and Labspec respectively, which are also a combination of a Lorentzian and Gaussian functions.

Figure 5a shows that due to peak broadening at the base of the 2D peak, which can occur as a result of doping [35, 84], strain variations [85, 86], substrate roughness [69], and increasing defect density [87] in graphene, a Lorentzian function cannot reliably fit both the peak shape and the peak tails. When comparing measurements from different spectrometers, the hardware in different instruments may also contribute to peak broadening [88]. As a (pseudo-)Voigt function is a (pseudo-)convolution of a Gaussian and Lorentzian function, any broadening at the base of the peak can be accounted for by an increasing Gaussian component, resulting in a more reliable fit of both the peak shape and the background. This is shown in Figure 5(b), where the pseudo-Voigt function produces a more convincing fit.

Due to the optimisation challenges associated with fitting peak data with a suboptimal peak function, different software packages may result in different peak fits. This is shown in Figure 5(c) where the distribution of Γ_{2D} values fitted from a variety of different software packages is almost identical using pseudo-Voigt functions, whereas it is quite inconsistent using Lorentzian functions.

The mean value of Γ_{2D} varied from 30.4 cm^{-1} to 33.6 cm^{-1} when using a Lorentzian function. The mean Γ_{2D} values reported across all software packages was (33.80 ± 0.08) cm^{-1} and (32 ± 1) cm^{-1} for pseudo-Voigt and Lorentzian fit functions, respectively. Considering the standard deviation in the Γ_{2D} values is 15× higher for Lorentzian fit functions, this demonstrates the consistency of pseudo-Voigt fit functions across different software packages. However, the distribution of I_{2D}/I_G values was more consistent for the different fit functions (Figure 5d), as such, peak intensity ratios fitted from different software packages should be more comparable than peak widths.

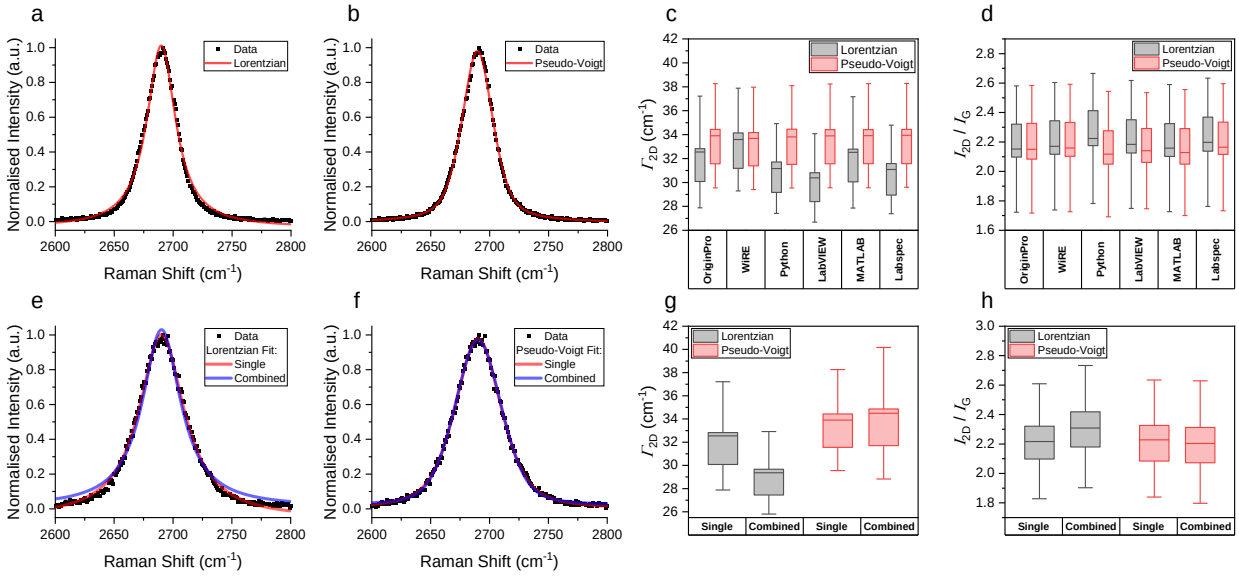

Figure 5: A Raman 2D peak fitted with a (a) Lorentzian and (b) pseudo-Voigt function using OriginPro 2020, and box plots of the (c) Γ_{2D} and (d) I_{2D}/I_G values that were fitted from the same Raman map using either a Lorentzian or a pseudo-Voigt function in a variety of different software packages. (e) A Raman 2D peak fitted with a Lorentzian where the 2D peak was either isolated from the spectrum and fitted independently (single) or all the Raman peaks (D, G, 2D) were fitted simultaneously (combined). (f) A Raman 2D peak fitted with a pseudo-Voigt where the 2D peak was either isolated from the spectrum and fitted independently or all the Raman peaks (D, G, 2D) were fitted simultaneously. Box plots of the (g) Γ_{2D} and (h) resulting I_{2D}/I_G values that were fitted from the same Raman map in OriginPro 2020 using either a single (independent) or combined (simultaneous) fitting methodology with Lorentzian and pseudo-Voigt functions. Each box in the box plots ((c), (d), (g) and (h)) shows the 25th, 50th (median) and 75th percentiles, and the whiskers show one standard deviation.

By plotting the absolute difference between the Lorentzian and pseudo-Voigt Γ_{2D} values as function of pseudo-Voigt Γ_{2D} values (Figure S5-25a), it was clear that different software packages fit increasingly broad 2D peaks very differently. While WiRE and OriginPro produced similar Lorentzian and pseudo-Voigt Γ_{2D} values regardless of the 2D peak width, the difference between the Lorentzian and pseudo-Voigt Γ_{2D} values increased as a function of 2D Peak width in Python, LabVIEW and MATLAB (up to 8 cm^{-1}) and decreased for Labspec. These results suggest that in the case of CVD-grown graphene, the pseudo-Voigt functions produce more reliable fits than Lorentzian functions, and pseudo-Voigt fits are also more consistent across different software packages when using the same fitting methodology.

Voigt lineshapes have also found to be more useful in fitting the symmetric Raman peaks of crystal structures [89]. Furthermore, pseudo-Voigt functions also allows the determination of the Gaussian component of the peak, which can be a useful additional metric for exploring variations in strain and doping [85, 86, 90]. Here, the 2D peak contained (36 ± 5) % Gaussian character across all of the CVD-grown graphene samples in this study (Table S3-23) and there did not appear to be a systematic difference in the m_u values between the edge and centre of the sample (Figure S5-23).

In combination with the peak fitting function, different peak fitting protocols can also directly affect the resulting $\Gamma_{2\mathrm{D}}$ values. Figure 5(e-f) demonstrate how the choice of either isolating a single peak before fitting or fitting all the peaks simultaneously can alter the shape of a fitted Lorentzian peak function. When fitting multiple peaks at the same time (*e.g.* D-, G-, and 2D Peaks), the fitting algorithm must simultaneously optimise for the other peaks in the spectrum and any variations in the background noise between them. Because of this, peak fitting with a simultaneous fitting procedure will be adversely affected if the background subtraction protocol is not adequately optimised. Unlike the Lorentzian function, the pseudo-Voigt function can accommodate broadening of the 2D Peak and produces a relatively consistent fit regardless of the choice in individual or simultaneous fitting (Figure 5 (e-f)). The robust nature of the pseudo-Voigt peak is shown in Figure 5(g-h), where the distribution of $\Gamma_{2\mathrm{D}}$ values and $I_{2\mathrm{D}}/I_{\mathrm{G}}$ values from Lorentzian peak fits were found to be dependent on whether an isolated or simultaneous peak fitting methodology was used, whereas the distribution of these values from pseudo-Voigt peak fits was relatively consistent for both protocols. This is further demonstrated in Figure S5-25(b), where the absolute difference between single Γ_{2D} fit values and combined Γ_{2D} fit values was found to increase as function of 2D peak width for a Lorentzian fit function, but was consistent for a pseudo-Voigt fit function.

These findings suggest that the variations in $\Gamma_{2\mathrm{D}}$ reported by the participants are due to the challenges associated with fitting the 2D Peak with a Lorentzian function, and how different software packages account for this. While the participants were asked to isolate each of the characteristic Raman peaks from the spectrum before fitting, some software packages do not allow such a granular control over the peak fitting protocol. The variations in $\Gamma_{2\mathrm{D}}$ that arise due to different software packages, peak fitting functions, and peak fitting protocols can result in unreliable and inconsistent Raman metrics for graphene. As many graphene applications will be critically dependent on robust analysis, such variations could dramatically increase the difficulty in developing and commercialising graphene technologies. To produce more reliable, consistent and comparable fitting of the Raman peaks in CVD graphene, the findings in this study demonstrate that a pseudo-Voigt function should be used to fit Raman 2D Peaks and each peak should be isolated from the spectrum before fitting.

4. Conclusion

CVD-grown graphene samples that were transferred onto Si/SiO_2 substrates were measured by 17 international participants consisting of National Measurement Institutes, Universities and industry. By comparing measurements performed on the same sample, contributions from the data analysis and the Raman measurement steps were separated. Comparisons of key Raman metrics such as $I_{2\mathrm{D}}/I_{\mathrm{G}}$ and Γ_{2D}, which are commonly described indicators for graphene in the graphene community, were performed. Whilst the peak fitting methods used in this study to calculate the I_{2D}/I_G peak intensity ratios and peak positions were consistent across all participants, there were significant variances in the absolute values of the I_{2D}/I_G ratios, and Γ_{2D}, in one case showing a variance of >200 % in I_{2D}/I_G. The $\mathrm{RMSE}_{I_{2\mathrm{D}}/I_{\mathrm{G}}}$ value from all participants was 0.031 for data analysis and 0.69 for measurements and the $\mathrm{RMSE}_{\Gamma_{2D}}$ value from all participants was 2.2 cm^{-1} for data analysis and 1.2 cm^{-1} for measurement, demonstrating how both the differences in measurement and the data analysis are important considerations for Raman spectroscopy analysis, depending on the measurands under investigation.

These sources of uncertainty can make developing and commercialising graphene technologies more challenging. However, we have shown that such variances can be substantially mitigated, in some cases by orders of magnitude, by following additional processes in addition to the protocol used here, as part of using a consistent and standardised procedure:

1) Performing a relative intensity calibration of the Raman spectrometer, using a certified reference material.
2) Use a pseudo-Voigt function, rather than a Lorentzian function, when fitting the Raman 2D-peak of CVD-grown graphene.
3) Peak fitting boundary parameters should be employed that ensure negative peak intensities, and therefore negative ratios, are not recorded.

Therefore, these important steps should be followed in addition to the original VAMAS project protocol (contained in the SI). These findings from this VAMAS project and protocol improvements will directly support the development of the ISO/IEC standard "*PWI 21356-2 - Nanotechnologies - Structural Characterisation of CVD-grown Graphene*".

Acknowledgements

PT, KRP, EL and AJP would like to thank the European Union's Horizon 2020 research and innovation program under Grant Agreement No, 881603 (Graphene Flagship Core 3) for funding. This work was conducted under VAMAS, as TWA 41 Project 1. We would also like to thank Cristina Giusca and Alex Shard, National Physical Laboratory (NPL) for discussions with regards to the manuscript. Hugo Kedoncuff acknowledges funding by the Danish Agency for Institutions and Educational Grants and thanks Anja Boisen and Tomas Rindzevicius of the IDUN Centre of Excellence (Denmark) for the use of their Raman microscope. Vaiva Nagyte and Cinzia Casiraghi acknowledge financial support from the EPSRC in the framework of the CDT Graphene NowNano. Luiz Gustavo Cançado acknowledges the Brazilian agencies CNPq, CAPES, FAPEMIG, and the MGgrafeno initiative (funded by Codemge). Raul Arenal acknowledges funding by the Spanish MICINN (PID2019-104739GB / 100 / AEI / 10.13039 / 501100011033) and by the Government of Aragon (project DGA E13-17R (FEDER, EU)). Sergio Jiménez-Sandoval thanks F. Rodríguez-Melgarejo for technical assistance.

Commercial equipment, instruments, and materials are identified in this paper in order to specify the experimental procedure adequately. Such identification is not intended to imply recommendation or endorsement by the National Institute of Standards and Technology or the United States government, nor is it intended to imply that the materials or equipment identified are necessarily the best available for the purpose. Work presented herein was performed, for a subset of the authors, as part of their official duties for the United States Government. Funding is hence appropriated by the United States Congress directly. The authors declare no competing interest.

References

[1] Novoselov K S, Jiang D, Schedin F, Booth T J, Khotkevich V V, Morozov S V and Geim A K Two-dimensional atomic crystals *Proceedings of the National Academy of Sciences of the United States of America* **102,** (2005) 10451-3
[2] Stankovich S, Dikin D A, Dommett G H B B, Kohlhaas K M, Zimney E J, Stach E A, Piner R D, Nguyen S T B T and Ruoff R S Graphene-based composite materials *Nature* **442,** (2006) 282-6
[3] Geim A K and Novoselov K S The rise of graphene *Nature Materials* **6,** (2007) 183-91
[4] Bonaccorso F, Sun Z, Hasan T and Ferrari A C Graphene photonics and optoelectronics *Nature Photonics* **4,** (2010) 611-22
[5] Shao Y, Wang J, Wu H, Liu J, Aksay I A and Lin Y 2010 Graphene based electrochemical sensors and biosensors: A review. In: *Electroanalysis*: John Wiley & Sons, Ltd) pp 1027-36
[6] Torrisi F, Hasan T, Wu W, Sun Z, Lombardo A, Kulmala T S, Hsieh G W, Jung S, Bonaccorso F, Paul P J, Chu D and Ferrari A C Inkjet-printed graphene electronics *ACS Nano* **6,** (2012) 2992-3006
[7] Raccichini R, Varzi A, Passerini S and Scrosati B The role of graphene for electrochemical energy storage *Nature Materials* **14,** (2015) 271
[8] Ferrari A C, Bonaccorso F, Fal'ko V, Novoselov K S, Roche S, Bøggild P, Borini S, Koppens F H L, Palermo V, Pugno N, Garrido J A, Sordan R, Bianco A, Ballerini L, Prato M, Lidorikis E, Kivioja J, Marinelli C, Ryhänen T, Morpurgo A, Coleman J N, Nicolosi V, Colombo L, Fert A, Garcia-Hernandez M, Bachtold A, Schneider G F, Guinea F, Dekker C, Barbone M, Sun Z, Galiotis C, Grigorenko A N, Konstantatos G, Kis A, Katsnelson M, Vandersypen L, Loiseau A, Morandi V, Neumaier D, Treossi E, Pellegrini V, Polini M, Tredicucci A, Williams G M, Hee Hong B, Ahn J H, Min Kim J, Zirath H, Van Wees B J, Van Der Zant H, Occhipinti L, Di Matteo A, Kinloch I A, Seyller T, Quesnel E, Feng X, Teo K, Rupesinghe N, Hakonen P, Neil S R T, Tannock Q, Löfwander T and Kinaret J Science and technology roadmap for graphene, related two-dimensional crystals, and hybrid systems *Nanoscale* **7,** (2015) 4598-810
[9] 229 I T and Nanotechnologies Nanotechnologies — Vocabulary — Part 13: Graphene and related two-dimensional (2D) materials *ISO/TS 80004-13:2017* (2017) 21
[10] Mas-Ballesté R, Gómez-Navarro C, Gómez-Herrero J and Zamora F 2011 2D materials: To graphene and beyond. In: *Nanoscale*: Royal Society of Chemistry) pp 20-30
[11] Novoselov K S, Fal'Ko V I, Colombo L, Gellert P R, Schwab M G and Kim K 2012 A roadmap for graphene. In: *Nature,* pp 192-200
[12] Novoselov K S, Mishchenko A, Carvalho A and Castro Neto A H 2D materials and van der Waals heterostructures *Science* **353,** (2016) aac9439
[13] Manzeli S, Ovchinnikov D, Pasquier D, Yazyev O V and Kis A 2017 2D transition metal dichalcogenides. In: *Nature Reviews Materials*: Nature Publishing Group) pp 1-15
[14] Soldano C, Mahmood A and Dujardin E 2010 Production, properties and potential of graphene. In: *Carbon,* pp 2127-50
[15] Wick P, Louw-Gaume A E, Kucki M, Krug H F, Kostarelos K, Fadeel B, Dawson K A, Salvati A, Vázquez E, Ballerini L, Tretiach M, Benfenati F, Flahaut E, Gauthier L, Prato M and Bianco A Classification framework for graphene-based materials *Angewandte Chemie - International Edition* **53,** (2014) 7714-8
[16] Colombo L D A, Casiraghi C, Kim M, Wallace R, Venugopal A. 2016 *Metrology and Diagnostic Techniques for Nanoelectronics,* pp 759-848
[17] Backes C, Higgins T M, Kelly A, Boland C, Harvey A, Hanlon D and Coleman J N Guidelines for exfoliation, characterization and processing of layered materials produced by liquid exfoliation *Chemistry of Materials* **29,** (2017) 243-55
[18] Mohan V B, Lau K t, Hui D and Bhattacharyya D Graphene-based materials and their composites: A review on production, applications and product limitations *Composites Part B: Engineering* **142,** (2018) 200-20

[19] Backes C, Abdelkader A M, Alonso C, Andrieux-Ledier A, Arenal R, Azpeitia J, Balakrishnan N, Banszerus L, Barjon J, Bartali R, Bellani S, Berger C, Berger R, Ortega M M B, Bernard C, Beton P H, Beyer A, Bianco A, Bøggild P, Bonaccorso F, Barin G B, Botas C, Bueno R A, Carriazo D, Castellanos-Gomez A, Christian M, Ciesielski A, Ciuk T, Cole M T, Coleman J, Coletti C, Crema L, Cun H, Dasler D, De Fazio D, Díez N, Drieschner S, Duesberg G S, Fasel R, Feng X, Fina A, Forti S, Galiotis C, Garberoglio G, García J M, Garrido J A, Gibertini M, Gölzhäuser A, Gómez J, Greber T, Hauke F, Hemmi A, Hernandez-Rodriguez I, Hirsch A, Hodge S A, Huttel Y, Jepsen P U, Jimenez I, Kaiser U, Kaplas T, Kim H K, Kis A, Papagelis K, Kostarelos K, Krajewska A, Lee K, Li C, Lipsanen H, Liscio A, Lohe M R, Loiseau A, Lombardi L, López M F, Martin O, Martín C, Martínez L, Martin-Gago J A, Martínez J I, Marzari N, Mayoral Á, McManus J, Melucci M, Méndez J, Merino C, Merino P, Meyer A P, Miniussi E, Miseikis V, Mishra N, Morandi V, Munuera C, Muñoz R, Nolan H, Ortolani L, Ott A K, Palacio I, Palermo V, Parthenios J, Pasternak I, Patane A, Prato M, Prevost H, Prudkovskiy V, Pugno N, Rojo T, Rossi A, Ruffieux P, Samorì P, Schué L, Setijadi E, Seyller T, Speranza G, Stampfer C, Stenger I, Strupinski W, Svirko Y, Taioli S, Teo K B K, Testi M, Tomarchio F, Tortello M, Treossi E, Turchanin A, Vazquez E, Villaro E, Whelan P R, Xia Z, Yakimova R, Yang S, Yazdi G R, Yim C, Yoon D, Zhang X, Zhuang X, Colombo L, Ferrari A C and Garcia-Hernandez M Production and processing of graphene and related materials *2D Materials* **7,** (2020)

[20] Legge D A J P D K R P D C A C M E Good Practice Guide No. 145: Characterisation of the Structure of Graphene *National Physical Laboratory, UK* **2,** (2017) 90-101

[21] Raman C V and Krishnan K S A new type of secondary radiation *Nature* **121,** (1928) 501-2

[22] GS Landsberg L M 1928 Eine neue Erscheinung bei der Lichtzerstreuung in Krystallen. In: *Die Naturwissenschaften*: Springer-Verlag) pp 557-8

[23] Thomsen C and Reich S Double resonant raman scattering in graphite *Physical Review Letters* **85,** (2000) 5214-7

[24] Casiraghi C, Ferrari A C and Robertson J Raman spectroscopy of hydrogenated amorphous carbons *Physical Review B - Condensed Matter and Materials Physics* **72,** (2005) 085401

[25] Reich S, Thomsen C and Maultzsch J 2007 *Carbon Nanotubes: Basic Concepts and Physical Properties*: Weinheim)

[26] Dresselhaus M S, Jorio A, Hofmann M, Dresselhaus G and Saito R Perspectives on carbon nanotubes and graphene Raman spectroscopy *Nano Letters* **10,** (2010) 751-8

[27] Jorio A, Saito R, Dresselhaus G and Dresselhaus M S 2011 Raman Spectroscopy in Graphene Related Systems. In: *Raman Spectroscopy in Graphene Related Systems*: Wiley- VCH)

[28] Ferrari A C and Basko D M Raman spectroscopy as a versatile tool for studying the properties of graphene *Nature Nanotechnology* **8,** (2013) 235-46

[29] Jorio A and Souza Filho A G Raman Studies of Carbon Nanostructures *Annual Review of Materials Research* **46,** (2016) 357-82

[30] Wu J B, Lin M L, Cong X, Liu H N and Tan P H Raman spectroscopy of graphene-based materials and its applications in related devices *Chemical Society Reviews* **47,** (2018) 1822-73

[31] Endo M, Iijima S and Dresselhaus M S 1997 *Carbon Nanotubes*: Pergamon)

[32] Bonaccorso F, Lombardo A, Hasan T, Sun Z, Colombo L and Ferrari A C Production and processing of graphene and 2d crystals *Materials Today* **15,** (2012) 564-89

[33] Ferrari A C, Meyer J C, Scardaci V, Casiraghi C, Lazzeri M, Mauri F, Piscanec S, Jiang D, Novoselov K S, Roth S and Geim A K Raman spectrum of graphene and graphene layers *Physical Review Letters* **97,** (2006) 187401

[34] Mohiuddin T M G, Lombardo A, Nair R R, Bonetti A, Savini G, Jalil R, Bonini N, Basko D M, Galiotis C, Marzari N, Novoselov K S, Geim A K and Ferrari A C Uniaxial strain in graphene by Raman spectroscopy: G peak splitting, Grüneisen parameters, and sample orientation *Physical Review B - Condensed Matter and Materials Physics* **79,** (2009) 205433

[35] Lee J E, Ahn G, Shim J, Lee Y S and Ryu S Optical separation of mechanical strain from charge doping in graphene *Nature Communications* **3,** (2012) 1024-8

[36] Zabel J, Nair R R, Ott A, Georgiou T, Geim A K, Novoselov K S and Casiraghi C Raman spectroscopy of graphene and bilayer under biaxial strain: Bubbles and balloons *Nano Letters* **12,** (2012) 617-21
[37] Silva D L, Campos J L E, Fernandes T F D, Rocha J N, Machado L R P, Soares E M, Miquita D R, Miranda H, Rabelo C, Vilela Neto O P, Jorio A and Cançado L G Raman spectroscopy analysis of number of layers in mass-produced graphene flakes *Carbon* **161,** (2020) 181-9
[38] Lucchese M M, Stavale F, Ferreira E H M, Vilani C, Moutinho M V O, Capaz R B, Achete C A and Jorio A Quantifying ion-induced defects and Raman relaxation length in graphene *Carbon* **48,** (2010) 1592-7
[39] Eckmann A, Felten A, Verzhbitskiy I, Davey R and Casiraghi C Raman study on defective graphene: Effect of the excitation energy, type, and amount of defects *Physical Review B - Condensed Matter and Materials Physics* **88,** (2013) 035426
[40] Pollard A J, Brennan B, Stec H, Tyler B J, Seah M P, Gilmore I S and Roy D Quantitative characterization of defect size in graphene using Raman spectroscopy *Applied Physics Letters* **105,** (2014)
[41] Cançado L G, Da Silva M G, Martins Ferreira E H, Hof F, Kampioti K, Huang K, Pénicaud A, Achete C A, Capaz R B and Jorio A Disentangling contributions of point and line defects in the Raman spectra of graphene-related materials *2D Materials* **4,** (2017)
[42] Neumann C, Reichardt S, Venezuela P, Drögeler M, Banszerus L, Schmitz M, Watanabe K, Taniguchi T, Mauri F, Beschoten B, Rotkin S V and Stampfer C Raman spectroscopy as probe of nanometre-scale strain variations in graphene *Nature Communications* **6,** (2015) 1-7
[43] Yang Y, Cheng G, Mende P, Calizo I G, Feenstra R M, Chuang C, Liu C W, Liu C I, Jones G R, Hight Walker A R and Elmquist R E Epitaxial graphene homogeneity and quantum Hall effect in millimeter-scale devices *Carbon* **115,** (2017) 229-36
[44] Ramesha G K and Sampath N S Electrochemical reduction of oriented Graphene oxide films: An in situ Raman spectroelectrochemical study *Journal of Physical Chemistry C* **113,** (2009) 7985-9
[45] Malard L M, Pimenta M A, Dresselhaus G and Dresselhaus M S Raman spectroscopy in graphene *Physics Reports* **473,** (2009) 51-87
[46] Tuinstra F, Koenig J L, F T, JL K, Tuinstra F, Koenig J L, F T and JL K Raman spectrum of graphite *The Journal of chemical physics* **53,** (1970) 1126-30
[47] Casiraghi C, Hartschuh A, Qian H, Pliscanec S, Georgia C, Fasoli A, Novoselov K S, Basko D M, Ferrari A C, Piscanec S, Georgi C, Fasoli A, Novoselov K S, Basko D M and Ferrari A C Raman spectroscopy of graphene edges *Nano Letters* **9,** (2009) 1433-41
[48] Cançado L G, Jorio A, Ferreira E H M, Stavale F, Achete C A, Capaz R B, Moutinho M V O, Lombardo A, Kulmala T S and Ferrari A C Quantifying defects in graphene via Raman spectroscopy at different excitation energies *Nano Letters* **11,** (2011) 3190-6
[49] Klar P, Lidorikis E, Eckmann A, Verzhbitskiy I A, Ferrari A C and Casiraghi C Raman scattering efficiency of graphene *Physical Review B - Condensed Matter and Materials Physics* **87,** (2013) 205435
[50] Ferreira H, Poma G, Acosta D R, Barzola-Quiquia J, Quintana M, Barreto L and Champi A Laser power influence on Raman spectra of multilayer graphene, multilayer graphene oxide and reduced multilayer graphene oxide Recent citations Laser power influence on Raman spectra of multilayer graphene, multilayer graphene oxide and reduced multilayer *IOP Conf. Series: Journal of Physics: Conf. Series* **1143,** (2018) 12020
[51] Tuschel D The Effect of Microscope Objectives on the Raman Spectra of Crystals *Spectroscopy* **32,** (2017) 14-23
[52] Gouadec G and Colomban P Raman Spectroscopy of nanomaterials: How spectra relate to disorder, particle size and mechanical properties *Progress in Crystal Growth and Characterization of Materials* **53,** (2007) 1-56

[53] Vidano R P, Fischbach D B, Willis L J and Loehr T M Observation of Raman band shifting with excitation wavelength for carbons and graphites *Solid State Communications* **39,** (1981) 341-4
[54] Piscanec S, Lazzeri M, Mauri F, Ferrari A C and Robertson J Kohn Anomalies and Electron-Phonon Interactions in Graphite *Physical Review Letters* **93,** (2004) 185503
[55] Paillet M, Parret R, Sauvajol J-L and Colomban P Graphene and related 2D materials: An overview of the Raman studies *Journal of Raman Spectroscopy* **49,** (2018) 8-12
[56] Malekpour H and Balandin A A Raman-based technique for measuring thermal conductivity of graphene and related materials *Journal of Raman Spectroscopy* **49,** (2018) 106-20
[57] 229 I T and Nanotechnologies Nanotechnologies — Structural characterization of graphene — Part 1: Graphene from powders and dispersions *ISO/TS 21356-1:202* (2021) 48
[58] Matthews M J, Pimenta M A, Dresselhaus G, Dresselhaus M S and Endo M Origin of dispersive effects of the Raman D band in carbon materials *Physical Review B - Condensed Matter and Materials Physics* **59,** (1999) R6585
[59] Casiraghi C, Pisana S, Novoselov K S, Geim A K and Ferrari A C Raman fingerprint of charged impurities in graphene *Applied Physics Letters* **91,** (2007) 233108
[60] Wang Y Y, Ni Z H, Yu T, Shen Z X, Wang H M, Wu Y H, Chen W and Wee A T S Raman studies of monolayer graphene: The substrate effect *Journal of Physical Chemistry C* **112,** (2008) 10637-40
[61] Li X, Cai W, An J, Kim S, Nah J, Yang D, Piner R, Velamakanni A, Jung I, Tutuc E, Banerjee S K, Colombo L and Ruoff R S Large-area synthesis of high-quality and uniform graphene films on copper foils *Science* **324,** (2009) 1312-4
[62] Hofmann S, Braeuninger-Weimer P and Weatherup R S 2015 CVD-enabled graphene manufacture and technology. In: *Journal of Physical Chemistry Letters*: American Chemical Society) pp 2714-21
[63] Suk J W, Kitt A, Magnuson C W, Hao Y, Ahmed S, An J, Swan A K, Goldberg B B and Ruoff R S Transfer of CVD-grown monolayer graphene onto arbitrary substrates *ACS Nano* **5,** (2011) 6916-24
[64] Li Z, Kinloch I A, Young R J, Novoselov K S, Anagnostopoulos G, Parthenios J, Galiotis C, Papagelis K, Lu C Y and Britnell L Deformation of Wrinkled Graphene *ACS Nano* **9,** (2015) 3917-25
[65] Thomson C, Establishing the Extent of Sample Damage and Safe Limits of Laser Exposure During Live Cell Analysis with Raman Spectroscopy, University of Strathclyde *PhD Thesis* (2021)
[66] Goldie S J, Bush S, Cumming J A and Coleman K S A Statistical Approach to Raman Analysis of Graphene-Related Materials: Implications for Quality Control *ACS Applied Nano Materials* **3,** (2020) 11229-39
[67] Krauss B, Lohmann T, Chae D H, Haluska M, Von Klitzing K and Smet J H Laser-induced disassembly of a graphene single crystal into a nanocrystalline network *Physical Review B - Condensed Matter and Materials Physics* **79,** (2009) 165428
[68] Babichev A V, Rykov S A, Tchernycheva M, Smirnov A N, Davydov V Y, Kumzerov Y A and Butko V Y Influence of Substrate Microstructure on the Transport Properties of CVD-Graphene *ACS Applied Materials and Interfaces* **8,** (2016) 240-6
[69] Banszerus L, Janssen H, Otto M, Epping A, Taniguchi T, Watanabe K, Beschoten B, Neumaier D and Stampfer C Identifying suitable substrates for high-quality graphene-based heterostructures *2D Materials* **4,** (2017) 025030
[70] Carozo V, Almeida C M, Ferreira E H M, Cançado L G, Achete C A and Jorio A Raman signature of graphene superlattices *Nano Letters* **11,** (2011) 4527-34
[71] Kim K, Coh S, Tan L Z, Regan W, Yuk J M, Chatterjee E, Crommie M F, Cohen M L, Louie S G and Zettl A Raman spectroscopy study of rotated double-layer graphene: Misorientation-angle dependence of electronic structure *Physical Review Letters* **108,** (2012) 246103

[72] Bayle M, Reckinger N, Huntzinger J R, Felten A, Bakaraki A, Landois P, Colomer J F, Henrard L, Zahab A A, Sauvajol J L and Paillet M Dependence of the Raman spectrum characteristics on the number of layers and stacking orientation in few-layer graphene *Physica Status Solidi (B) Basic Research* **252,** (2015) 2375-9
[73] Martins Ferreira E H, Moutinho M V O, Stavale F, Lucchese M M, Capaz R B, Achete C A and Jorio A Evolution of the Raman spectra from single-, few-, and many-layer graphene with increasing disorder *Physical Review B - Condensed Matter and Materials Physics* **82,** (2010)
[74] Yoon D, Moon H, Son Y W, Choi J S, Park B H, Cha Y H, Kim Y D and Cheong H Interference effect on Raman spectrum of graphene on SiO2 /Si *Physical Review B - Condensed Matter and Materials Physics* **80,** (2009) 125422
[75] Gupta A K, Russin T J, Gutiérrez H R and Eklund P C Probing graphene edges via raman scattering *ACS Nano* **3,** (2009) 45-52
[76] Graf D, Molitor F, Ensslin K, Stampfer C, Jungen A, Hierold C and Wirtz L Spatially resolved raman spectroscopy of single- and few-layer graphene *Nano Letters* **7,** (2007) 238-42
[77] Ray K G and McCreery R L Simplified calibration of instrument response function for Raman spectrometers based on luminescent intensity standards *Applied Spectroscopy* **51,** (1997) 108-16
[78] Lee T, Mas'Ud F A, Kim M J and Rho H Spatially resolved Raman spectroscopy of defects, strains, and strain fluctuations in domain structures of monolayer graphene *Scientific Reports* **7,** (2017) 1-8
[79] NIST, Relative Intensity Correction Standards for Fluorescence and Raman Spectroscopy, *https://www.nist.gov/programs-projects/relative-intensity-correction-standards-fluorescence-and-raman-spectroscopy*, 8th July 2021
[80] Choquette S J, Etz E S, Hurst W S, Blackburn D H and Leigh S D Relative intensity correction of Raman spectrometers: NIST SRMs 2241 through 2243 for 785 nm, 532 nm, and 488 nm/514.5 nm excitation. *Applied spectroscopy* **61,** (2007) 117-29
[81] Piao Y, Simpson J R, Streit J K, Ao G, Zheng M, Fagan J A and Hight Walker A R Intensity Ratio of Resonant Raman Modes for (n,m) Enriched Semiconducting Carbon Nanotubes *ACS Nano* **10,** (2016) 5252-9
[82] ASTM, ASTM E1840 - 96 Standard Guide for Raman Shift Standards for Spectrometer Calibration(2014)
[83] Schreier F An assessment of some closed-form expressions for the Voigt function III: Combinations of the Lorentz and Gauss functions *Journal of Quantitative Spectroscopy and Radiative Transfer* **226,** (2019) 87-91
[84] Berciaud S, Ryu S, Brus L E and Heinz T F Probing the Intrinsic Properties of Exfoliated Graphene: Raman Spectroscopy of Free-Standing Monolayers *Nano Letters* **9,** (2009) 246-352
[85] Eckmann A, Park J, Yang H, Elias D, Mayorov A S, Yu G, Jalil R, Novoselov K S, Gorbachev R V, Lazzeri M, Geim A K and Casiraghi C Raman fingerprint of aligned graphene/h-BN superlattices *Nano Letters* **13,** (2013) 5242-6
[86] Kunc J and Rejhon M Raman 2D Peak Line Shape in Epigraphene on SiC *Applied Sciences* **10,** (2020) 2354
[87] Shlimak I, Butenko A, Kogan E and Kaveh M Irradiation-induced broadening of the Raman spectra in monolayer graphene *Journal of Applied Physics* **126,** (2019) 194302
[88] Váczi T A new, simple approximation for the deconvolution of instrumental broadening in spectroscopic band profiles. *Applied spectroscopy* **68,** (2014) 1274-8
[89] Yuan X and Mayanovic R A An Empirical Study on Raman Peak Fitting and Its Application to Raman Quantitative Research *Applied Spectroscopy* **71,** (2017) 2325-38
[90] Huang C H, Lin H Y, Huang C W, Liu Y M, Shih F Y, Wang W H and Chui H C Probing substrate influence on graphene by analyzing raman lineshapes *Nanoscale Research Letters* **9,** (2014) 1-5